Iron is critical for mucosal-associated invariant T cell metabolism and effector functions

Eimear K. Ryan[*], Christy Clutter[†,‡], Conor De Barra[*], Benjamin J. Jenkins[¶], Simon O'Shaughnessy[||], Odhran Ryan[*,††], Chloe McKenna[*], Helen Heneghan[††], Fiona Walsh[*], David K. Finlay[||,‡‡], Linda V. Sinclair[¶¶], Nicholas Jones[¶], Daniel T. Leung[†,‡,], Donal O'Shea[*,††] and Andrew E. Hogan[*]

Affiliations: [*]Kathleen Lonsdale Institute for Human Health Research, Maynooth University, Maynooth, Co Kildare. Ireland. [†]Division of Infectious Diseases, Department of Internal Medicine, University of Utah School of Medicine, Salt Lake City, Utah, United States of America. [‡]Division of Microbiology and Immunology, Department of Pathology, University of Utah School of Medicine, Salt Lake City, Utah, United States of America. [¶]Institute of Life Science, Swansea University Medical School, Swansea, United Kingdom. [||]Trinity Biomedical Sciences Institute, School of Biochemistry and Immunology, Trinity College Dublin, Dublin 2, Ireland. [††]St Vincent's University Hospital & University College Dublin, Dublin 4, Ireland. [‡‡]School of Pharmacy and Pharmaceutical Sciences, Trinity College Dublin, Dublin 2 Ireland. [¶¶]Division of Cell Signaling and Immunology, School of Life Sciences, University of Dundee, United Kingdom.

Address for correspondence:
Dr Andrew Hogan –
Email: Andrew.E.Hogan@mu.ie
Address: Biosciences Building,
Maynooth University, Maynooth,
Co. Kildare, Ireland.
Phone: +35317086118

Running title: Iron is critical for MAIT cell effector function

Keywords: Mucosal associated invariant T cells, Metabolism, Iron

Abstract

Mucosal Associated Invariant T (MAIT) cells are a population of innate T cells which play a critical role in host protection against bacterial and viral pathogens. Upon activation, MAIT cells can rapidly respond via both T cell receptor dependent and independent mechanisms, resulting in robust cytokine production. The metabolic and nutritional requirements for optimal MAIT cell effector responses are still emerging. Iron is an important micronutrient, and is essential for cellular fitness, in particular cellular metabolism. Iron is also critical for many pathogenic microbes, including those which activate MAIT cells. However, iron has not been investigated with respect to MAIT cell metabolic or functional responses. In this study we show that human MAIT cells require exogenous iron, transported via CD71 for optimal metabolic activity in MAIT cells, including their production of ATP. We demonstrate that restricting iron availability by either chelating environmental iron or blocking CD71 on MAIT cells results in impaired cytokine production and proliferation. These data collectively highlight the importance of a CD71-iron axis for human MAIT cell metabolism and functionality, an axis which may have implications in conditions where iron availability is limited.

Key Points

- Activated MAIT cells increase iron uptake via CD71
- MAIT cell metabolism and functionality is dependent on a CD71-iron axis

Introduction

Mucosal Associated Invariant T (MAIT) cells are a population of non-MHC restricted T cells that are important in the immune defence against bacterial and viral infections(1-5). MAIT cells are rapidly responding T cells that are capable of producing multiple cytokines upon activation such as IFN-γ, TNF and IL-17(1, 6). MAIT cells are activated when their invariant T cell receptor (TCR) recognises bacterial riboflavin derivatives presented on the MHC like molecule MR1(5, 6). In contrast, they can also be activated in a TCR- independent manner, via stimulation with cytokines such as IL-18(7, 8). Recently, several studies have highlighted the importance of metabolism for MAIT cell functional responses(9). Our group and others have demonstrated that MAIT cells are reliant on glycolysis to support their production of IFNγ and Granzyme B(10-12), whereas IL-17 production by MAIT cells has been linked to mitochondrial metabolism(13, 14). However, our knowledge of the nutritional requirements of MAIT cells remains limited.

Iron is an essential trace element for all multicellular organisms, and is critical for a range of physiological processes including oxygen transport and energy production(15). Iron is also critical for the majority of microorganisms, and successful iron sequestration is required to establish infection(16). Iron availability is regulated by the liver-derived hormone, hepcidin. Increased hepcidin production occurs in response to infection and inflammation, and results in reduced iron availability, a mechanism of host protection(17, 18). However, previous studies have demonstrated that conventional T cell responses are negatively impacted by low iron levels, with reduced proliferation and effector functions(19, 20). Whether MAIT cells require iron for their metabolic processes and effector responses is currently unknown.

In the current study, we demonstrate that MAIT cells upregulate their expression of the transferrin receptor, CD71, upon activation, correlating with a significant increase in the uptake of transferrin-bound iron. *In silico* analysis of the MAIT cell proteome reveals that MAIT cells increase their overall iron content upon activation. We demonstrate that MAIT cell metabolism is limited, and the metabolic profile altered, under iron-deplete conditions, and this is associated with a robust reduction in ATP

92 levels. Finally, we demonstrate that extracellular iron-restriction impairs MAIT cell
93 functional responses, lending to a reduced proliferative capacity and diminished
94 cytokine production. Collectively our data pinpoint MAIT cells as another player in the
95 iron tug-of-war between pathogenic invaders and host immunity.
96

Materials & methods

Study Cohorts & Ethical Approval. A total cohort of healthy 30 adult donors were recruited. Inclusion criteria included ability to give informed consent, 18-65 years of age, BMI<28, no current or recent (<2 weeks) infection. Ethical approval was obtained from both St Vincent's University Medical Ethics Committee and Maynooth University Ethics Committee.

Preparation of Peripheral Blood Mononuclear Cells (PBMC) and Flow Cytometric Analysis. PBMC samples were isolated, using SepMate isolation tubes, by density-centrifugation over Lymphoprep (both STEMCELL Technologies), from fresh human-peripheral blood samples. Cell viability was determined using eBioscience Fixable Viability Dye (eFluor506), and MAIT cells were phenotyped using specific extracellular monoclonal antibodies (Miltenyi Biotec and BioLegend), namely CD3, CD161, TCRVα7.2, and CD71. Where appropriate, cells were fixed and permeabilized according to manufacturer guidelines, using the True-Nuclear Transcription Factor Buffer set (BioLegend). Cell populations were identified using an Attune NXT flow cytometer and analysed using FlowJo version 10.8.2 (TreeStar). Results are expressed either as a percentage of the parent population as indicated and determined using flow minus one (FMO) and unstained controls; or as the mean fluorescence intensity (MFI) of the relevant population.

MAIT Cell Transferrin Uptake Assay. PBMC ($2x10^6$/ml) were activated using CD3/CD28 TCR Dynabeads (Gibco) and IL-18 (50ng/ml) or cytokine alone (IL-12/IL-18 both 50ng/ml) for 18 hours as indicated. Cells were rested in serum-free HPLM with 5% BSA for 2 hours. Cells were then washed in serum-free HPLM with 0.5% BSA and incubated with 5μg/ml Transferrin-AlexaFluor647 (Invitrogen) for 10 minutes at 37°C. Holo-transferrin (500μg/ml, Sigma-Aldrich) was used to competitively control for transferrin-uptake. Cells were washed in ice-cold HPLM with 0.5% BSA to stop membrane trafficking. Cells were then stained for viability, and MAIT cells or conventional T cells were labelled for extracellular markers, to be analysed by flow cytometry.

***In Silico* Proteomic Analysis.** Publicly available proteomic data set of MAIT cells were downloaded from PRIDE accession number PXD041544 (https://www.ebi.ac.uk/pride/archive/projects/PXD041544). A list of human iron interacting proteins was provided by Andreini et al(21). Using the protocol from Teh and colleagues(22), the list of human iron interacting proteins was compared and aligned against the complete list of proteins detected in the human MAIT cell proteomic dataset. Matches were extracted and listed in Table S1. To estimate the iron atom counts per protein species the copy number value of each iron interacting protein was multiplied by the iron atom counts per protein. If available, iron atom counts per protein were obtained using the Uniprot database cofactor information for each protein. Where iron counts were not available, estimates of iron usage per protein species were assumed to be 1 atom for heme and iron interacting proteins and 2 atoms for FE-S cluster interacting proteins. The total number of iron atoms required per cell was calculated as the sum of iron atoms required by each protein species.

MAIT Cell SCENITH Assay. Fresh PBMC (2 x 10^6/mL) were activated using CD3/CD28 TCR Dynabeads, and IL-18 (50ng/mL) for 18 hours. Cells were seeded into a 96-well plate, and treated as a control, or with 2-Deoxy-D-Glucose (100mM), Oligomycin (1μM), or both. Following incubation at 37°C for 15 minutes, cells were treated with Puromycin (11μM) and incubated for a further 25 minutes. Cells were washed with ice-cold PBS to stop puromycin incorporation. Cells were then stained for viability. MAIT cells were stained for extracellular markers and fixed, as outlined above. Staining of puromycin was achieved using anti-puromycin monoclonal antibody (AlexaFluor488, Sigma), in permeabilization buffer (BioLegend).

MAIT Cell Seahorse Assay. Purified MAIT cells (IL-2 expanded) were activated using CD3/CD28 TCR Dynabeads, and IL-18 (50ng/mL) for 18 hours in the absence or presence of DFO (200μM, Sigma) and metabolic analysis was carried out using the Seahorse Extracellular Flux Analyzer XFe96 (Agilent). MAIT cells were resuspended in phenol red-free RPMI media containing 10mM glucose, 2mM glutamine and 1mM pyruvate (Agilent) and plated onto a Cell-Tak (Corning) coated microplate for

adhesion. Respiratory parameter (mitochondrial and glycolytic) were measured using OCR (pmole/min) and ECAR (mpH/min), respectively, using injections of oligomycin (1μM), FCCP (1μM), rotenone and antimycin A (both 1μM) and monensin (20μM) (All Sigma). Metabolic parameters were calculated as per well-established protocols(23, 24).

MAIT Cell Mitochondrial Analysis. Fresh PBMC (2 x 10^6 /mL) were activated using CD3/CD28 TCR Dynabeads, and IL18 (50ng/mL) for 18 hours, in the absence or presence of DFO (200μM, Sigma). Cells were seeded into a 96-well plate, and washed in serum-free buffer. Cells were then stained for viability as outlined above, and MAIT cells were stained for extracellular markers. Cells were then washed, and stained with Mitotracker Deep Red FM (50μM, ThermoFisher Scientific) and Mitotracker Green (50μM, ThermoFisher Scientific) in PBS, and incubated for 1 hour at 37°C. Cells were subsequently analysed by flow-cytometric analysis.

MAIT Cell ATP Assay. Interleukin-2 expanded MAIT cells (1x10^6/ml) were stimulated using CD3/CD28 TCR Dynabeads, and IL18 (50ng/mL) for 18 hours. ATP levels were measured using a luminescence ATP assay kit (abcam). Reagents in the kit were reconstituted as per manufacturer's instructions. A standard curve was also prepared as per the kit's the instructions. MAIT cells were harvested and washed with PBS. 100μL of resuspended MAIT cells was added to a black walled, clear bottomed plate. 50μL of detergent was added to each well and the plate was placed on an orbital shaker for 5 minutes at 600-700 rpm. 50μl of substrate solution was added and the plate was returned to the orbital shaker for 5 minutes at 600-700 rpm. The plate was then covered and placed in the dark for 10 minutes before luminescence was measured on a multimode plate reader (CLARIOstar).

MAIT Cell Functional Analysis. IL-2 expanded MAIT cells were activated using CD3/CD28 TCR Dynabeads and IL-18 (50ng/ml) for 18 hours in the absence or presence of DFO (100μM), or anti-CD71 monoclonal antibody (20μg/mL). An appropriate IgG

isotype control was used in blocking experiments. After 18 hours, culture supernatants were assessed for IFNγ, IL-17 or IL-26 levels using ELISA.

MAIT Cell *E. coli* stimulation assay. Freshly isolated MAIT cells were incubated with 20μg/mL anti-CD71 monoclonal antibody (Invitrogen) for 1 hour. Meanwhile, THP-1 cells (ATCC TIB-202) were pre-pulsed for 1 hour with fixed *E. coli* (DH5α) at an MOI of 100. At the end of an hour, representative THP-1 cells with and without *E. coli* were counted and titrated to match the number of MAIT cells at a 1:1 ratio, and MAIT cells were cocultured with THP-1 overnight. Four hours before staining for flow cytometry, cells were centrifuged and resuspended in media containing brefeldin A (Invitrogen). Intracellular cytokine (IFNγ and Granzyme B) levels were assessed using flow cytometry (Cytex Aurora) .

MAIT Cell Proliferation Analysis. Fresh PBMC (1 x 10^6 /ml) were stimulated for 24 hours with 5 μg/mL of 5-ARU and 100 μM of Methylglyoxal, in the absence or presence of DFO (200μM) and $FeSO_4 \bullet 7H_2O$ (200μM, Sigma). After 24 hours, culture media was replaced with fresh culture media containing IL-2 (6.8 ng/mL). After 48 hours, culture media was replaced with fresh culture media containing IL-2 (34 ng/ mL) . On day 5, absolute cell numbers were determined using flow cytometric analysis of MAIT cell frequencies, and total cell counts.

Statistics. Statistical analysis was completed using Graph Pad Prism 6 Software (USA). Data is expressed as SEM. Distribution was assessed using Shapiro-Wilk test. We determined differences between two groups using Student T-test (paired or unpaired) or Wilcoxon Signed-Rank test where appropriate. Analysis across 3 or more groups was performed using ANOVA with multiple measures. Correlations were determined using linear regression models and expressed using Pearson or Spearman's rank correlation coefficient, as appropriate. P values were expressed with significance set at <0.05.

RESULTS

MAIT cells increase their expression of the transferrin transporter CD71 upon activation.

First we demonstrate that MAIT cells from PBMC increase transferrin receptor (CD71) surface expression in response to TCR/IL18 stimulation but not cytokine alone. (Fig1 A-D & Figure S1). We then compared CD71 expression on activated MAIT cells and activated conventional T cells and noted higher CD71 expression on conventional T cells (Figure 1E). Next, we investigated whether MAIT cells altered their CD71 expression under restricted iron conditions. In order to do this, we limited iron availability in our culture system using the iron chelator deferoxamine (DFO) which did not impact MAIT cell viability at 18 hours (Figure S2). Resting MAIT cells do not have high levels of CD71 expression however upon iron depletion both the proportion of MAIT cells which express CD71 and the amount of CD71 expressed was increased , and this was also evident in TCR/IL18 activated MAIT cells (Figure 1F-H & Figure S2), suggesting a compensatory mechanism to support iron uptake. Next, we investigated the functionality of CD71, using a transferrin uptake assay, and show increased transferrin uptake (both % of MAIT cells and MFI) by activated MAIT cells, and again noted higher uptake by activated conventional T cells (Figure 1I-M). Finally, we demonstrate a linear relationship between CD71 expression and transferrin uptake in activated MAIT cells (Figure 1N).

In silico analysis of the MAIT cell proteome reveals increased iron content upon activation.

To assess the iron requirements of MAIT cells, we performed *in silico* pathway analysis of a previously published proteomics data-set(12). We found that IL-2 expanded MAIT cells express high basal expression of ferritin, the protein responsible for iron storage, which is reduced upon activation (Figure 2A-B). Next, we determined the number of iron-interacting proteins in MAIT cells, and identified 135 proteins in total, representative of 2.3% of the total proteome (Figure 2C & Table S1). Pathway analysis revealed these proteins were intrinsic to many processes, including a major involvement in cellular metabolism (Figure 2D). Using a recently published

algorithm(22) which determines cellular iron content, based on number of iron containing proteins multiplied by the number of iron atoms per protein, we determined the predicted iron content from the MAIT cell dataset , and show an approximately $1x10^7$ iron atoms in MAIT cells, increasing significantly upon activation (Figure 2E). Finally, we found that the iron content of MAIT cells is associated with Heme and iron-sulphur clusters (Figure 2F-G).

Iron is a critical co-factor for MAIT cell metabolism.

We next investigated if limiting iron availability in our culture system using the iron chelator deferoxamine (DFO) impacted MAIT cell metabolism. Using protein translation as functional readout of metabolism, we demonstrate that activated MAIT cells significantly increase protein translation after stimulation (Figure 3A-B), and protein translation is limited when MAIT cells are activated in the presence of DFO (Figure 3C-D & Figure S2). A recently published method, SCENITH(25), demonstrated that the measurement of protein translation, paired with the use of metabolic inhibitors such as 2-deoxyglucose (2DG) and oligomycin, allows for metabolic analysis of cells at a single cell level. Using the SCENITH approach (Figure S2), we demonstrate that iron-restricted MAIT cells increase their dependency on glucose metabolism (Figure 3E), and this was paired with a decreased capacity to undergo oxidative-linked metabolic processes (Figure 3F). With this reduction in oxidative metabolism, we next examined the impact of limiting iron on the mitochondrial phenotype, and observed modest increases in both mitochondrial mass (MitoTracker Green) and membrane potential (MitoTracker Deep Red) (Figure 3G-H). To confirm these observations we next investigated the impact of iron restriction via DFO treatment on MAIT cell metabolism using extracellular flux analysis and noted strong inhibition in the rates of oxidative phosphorylation (Figure 3I-J). We also noted reduced rates of glycolysis (Figure S3). Furthermore, when we tested the mitochondrial capacity of MAIT cells using the FCCP treatment we observed a striking reduction with DFO treatment (Figure 3K). Finally, we examined the impact of low iron availability, using a monoclonal antibody to block CD71, on ATP levels in MAIT cells, and demonstrate that iron restriction limits ATP production. (Figure 3L), a finding supported by our Seahorse analysis (Figure S3).

MAIT cell functional responses require extracellular iron

We next investigated if MAIT cells require extracellular iron for their functional responses. We assessed the impact of DFO treatment on MAIT cell in PBMC ability to produce IFNγ via flow cytometry and observed a reduction with iron restriction (Figure 4A). Next we investigated the impact of DFO on the cytokine responses of isolated MAIT cells and show reductions in IFNγ, IL-17 and IL-2 levels (Figure 4B-D). To confirm the impact of low iron availability on MAIT cell IFNγ production, we switched our approach to block CD71 and again demonstrate significant reductions in IFNγ levels (Figure 4E). We next assessed the impact of limiting iron availability on MAIT cell production of the antimicrobial cytokine IL-26, and demonstrate significantly reduced levels with CD71 blockade (Figure 4F). We next assessed the impact of iron restriction via CD71 blockade on freshly isolated MAIT cell responses to THP-1 cells infected with *E. Coli* and demonstrated significant reductions in both IFNγ and granzyme B production (Figure 4G-H). With the noted impact of iron restriction on MAIT cell metabolism, we sought to assess the impact of long-term iron restriction on MAIT cell proliferative capacity and viability. We first show that MAIT cells proliferation is inhibited with the addition of the ATP synthase inhibitor oligomycin (Figure 4I), and then demonstrated that MAIT cells fail to proliferate under low iron conditions, and this was paired with a significant reduction in cell viability, which was significantly improved with the addition of FeSO4, which bypasses CD71 (Figure 4J-K).

Discussion.

MAIT cells are a subset of unconventional T cells capable of rapidly responding to stimulation, producing cytokines, lytic molecules and proliferating(26). MAIT cells are key mediators of host protection against many bacterial and viral pathogens(2, 3, 27-29). Immune responses are metabolically intense processes, with significant energy demands required to support *de novo* generation of biosynthetic intermediates(30). The metabolic processes and nutrient requirements that govern MAIT cell effector responses are rapidly emerging but still incomplete(10-13, 31). Iron is an essential microelement and is critical for almost all living organisms, including humans and the majority of microbes(15). Iron plays a critical role in cellular metabolism and energy

production, and is vital for conventional T cell immunity(19, 20). The iron requirements of MAIT cells are unknown. In this study, we show that MAIT cell metabolism and functional responses, namely cytokine production and proliferation, are governed by extracellular iron availability. We show that activated MAIT cells increase their expression of CD71, the transferrin receptor, and that iron-restriction significantly diminishes MAIT cell protein translation and ATP production. Consequently, MAIT cells present with a reduced capacity to proliferate, and diminished production of several cytokines central to MAIT cell host protective function.

The majority of bioavailable iron in the circulation is bound to transferrin which is taken into cells via the transferrin receptor TfR1, also known as CD71(32). We first examined MAIT cells for the expression of CD71 and found low basal expression but significant increases in expression after stimulation with TCR beads/IL-18 but not IL-12/IL-18 suggesting a TCR dependency, this supports our previous study which highlighted CD71 as a MYC target, which is an important transcription factor upregulated by TCR stimulation in MAIT cells(12). Previous studies have reported similar activation induced increases in CD71 expression on activated T cells and NK cells(33, 34). Interestingly, a missense mutation in TFRC, the gene encoding CD71, resulted in immunodeficiency underpinned by defective T cells(35). In line with increased CD71 expression, we observed increased uptake of transferrin by activated MAIT cells, similar to that reported in both conventional CD4+ and CD8+ T cells(36). MAIT cells are primarily CD8+, and recently it was demonstrated that CD8 receptor expression was critical for optimal TCR driven responses in MAIT cells(37). In a recent study by Teh and colleagues, they reported greater iron dynamics in CD8+ T cells compared to CD4+ T cells, which is supported by proteomic data from Howden et al where they demonstrated that CD8+ T cells express more CD71 than CD4+ T cells(33). To investigate the iron dynamics of MAIT cells we performed *in silico* analysis of our publicly available proteomic dataset(12). We found that MAIT cells decrease their levels of ferritin, suggesting mobilization of iron stores(38). Using the approach introduced by Teh et al for determining cellular iron content based on proteomic analysis(22) , we found that MAIT cells contain 135 proteins with iron binding sites

and significantly increase their predicted iron content upon activation, similar to that observed in conventional T cell subsets(22).

Pathway analysis of the 135 proteins with iron binding sites present in MAIT cells highlighted cellular metabolism as a major process central to these proteins. Similarly, Teh and colleagues found that the majority of intracellular iron in T cells was utilized in oxidative phosphorylation(22). Therefore, we next assessed the impact of altered iron availability on MAIT cell metabolism and functional responses. We used two different approaches to limit MAIT cell access to extracellular iron; (1) we utilized the iron chelator deferoxamine (DFO) which removes iron from ferritin(39), (2) we utilized a monoclonal antibody specific for CD71 with blocking activity(40). To assess the impact of low iron availability on MAIT cell metabolism we used two different approaches, Seahorse extracellular flux analysis and a recently published method SCENITH, which monitors rapid changes in protein translation paired with a series of metabolic inhibitors to profile cellular metabolism at a single cell level(25). Using SCENITH, we found that MAIT cells significantly increase protein translation upon activation. This supports our recent publication where we demonstrated significant increases in protein content in activated MAIT cells(12). In the presence of DFO, protein translation was reduced in activated MAIT cells, suggesting that iron supports global MAIT cell metabolism. This was confirmed by our Seahorse data which showed reduced rates of glycolysis and to a greater extent reduced rates of OxPhos. Similarly in activated NK cells, treatment with DFO resulted in reduced cell size, indicative of reduced protein content and metabolism(34). Paired with reduced protein translation, limited iron availability also reduced the oxidative capacity of activated MAIT cells, suggesting altered mitochondria, similar to that reported in conventional T cells by Frost and colleagues(20). In the same study by Frost *et al*, iron deficiency resulted in reduced ATP production and an accumulation of dysregulated mitochondria in CD8+ T cells(20). We observed only modest changes in mitochondrial phenotype, but note the longer timeframe in the study by Frost *et al* compared to our overnight timepoint. We did however find reduced mitochondrial capacity and ATP levels in MAIT cells activated in the presence of limited iron availability.

Iron is critical for the majority of commensal and pathogenic bacteria, and during infection, in response to inflammation, the host restricts the accessibility of iron as a protective measure. Many pathogenic bacteria synthesize iron chelators called siderophores to scavenge host iron, resulting in an iron tug-o-war(41). One of the major roles for MAIT cells is mediating host protection against bacteria(27, 42-44). Interestingly, several bacteria which elicit MAIT cell responses *in vivo*, such as *Salmonella typhimurium*(45), *Klebsiella pneumoniae(46)* and *Legionella longbeachae*(47) utilize siderophores as a virulence factor(48-50). Therefore, we investigated if MAIT cells need iron for their effector functions, the primary of which is cytokine production. Previously, we had found IFNγ the most abundant cytokine produced by MAIT cells, and here we demonstrate that limiting iron availability limits the levels of IFNγ secreted in response to either TCR stimulating beads or THP-1 cells infected with *E. coli*. Similarly, in a model of hepcidin driven hypoferremia, antigen specific CD8 T cells produced less IFNγ than in control mice, highlighting the importance of iron for conventional T cell responses. Interleukin-26 is cytokine with direct antimicrobial activity produced by MAIT cells, and part of MAIT cell responses to infection in the lung(28). We found that IL-26 production by MAIT cells was also reduced under limited iron conditions. Another key effector function required for MAIT cell host defence is the ability to proliferate(51). We found that under iron restriction MAIT cells failed to proliferate, likely linking into the reduced metabolism observed. In CD4 T cells, iron was also required for proliferation, and the authors linked this failure to altered mitochondrial metabolism(19), supporting our data which demonstrated significant reduction in MAIT cell proliferation with ATP synthase inhibition. In summary our study highlights the importance of iron for MAIT cell metabolic and functional responses, and may have implications in conditions where iron availability is limited.

Contributors Statement: EKR, CC, CDB, BJJ and CMcK performed the experiments, carried out analysis and approved the final manuscript as submitted. SOS and DKF performed proteomic analysis, helped with study design, analysis and approved the final manuscript as submitted. OR, HH and DOS recruited study participants and helped with study design, analysis and approved the final manuscript as submitted. DOS, FW, DTL, NJ, LVS & AEH conceptualized and designed the study, analyzed the data, drafted the manuscript, and approved the final manuscript as submitted.

Funding Source: This study is supported by the Kathleen Lonsdale Institute for Human Health Research. Financial support for the Attune NxT was provided to Maynooth University Department of Biology by Science Foundation Ireland (16/RI/3399).

Financial Disclosure: The authors declare no financial relationships relevant to this article to disclose.

Competing Interest: The authors declare no conflict of interest.

REFERENCES

1. Godfrey, D. I., H. F. Koay, J. McCluskey, and N. A. Gherardin. 2019. The biology and functional importance of MAIT cells. *Nat Immunol* 20: 1110-1128.
2. Le Bourhis, L., E. Martin, I. Péguillet, A. Guihot, N. Froux, M. Coré, E. Lévy, M. Dusseaux, V. Meyssonnier, V. Premel, C. Ngo, B. Riteau, L. Duban, D. Robert, S. Huang, M. Rottman, C. Soudais, and O. Lantz. 2010. Antimicrobial activity of mucosal-associated invariant T cells. *Nat Immunol* 11: 701-708.
3. van Wilgenburg, B., I. Scherwitzl, E. C. Hutchinson, T. Leng, A. Kurioka, C. Kulicke, C. de Lara, S. Cole, S. Vasanawathana, W. Limpitikul, P. Malasit, D. Young, L. Denney, M. D. Moore, P. Fabris, M. T. Giordani, Y. H. Oo, S. M. Laidlaw, L. B. Dustin, L. P. Ho, F. M. Thompson, N. Ramamurthy, J. Mongkolsapaya, C. B. Willberg, G. R. Screaton, P. Klenerman, and S.-H. consortium. 2016. MAIT cells are activated during human viral infections. *Nature communications* 7: 11653.
4. Treiner, E., L. Duban, S. Bahram, M. Radosavljevic, V. Wanner, F. Tilloy, P. Affaticati, S. Gilfillan, and O. Lantz. 2003. Selection of evolutionarily conserved mucosal-associated invariant T cells by MR1. *Nature* 422: 164-169.
5. Kjer-Nielsen, L., O. Patel, A. J. Corbett, J. Le Nours, B. Meehan, L. Liu, M. Bhati, Z. Chen, L. Kostenko, R. Reantragoon, N. A. Williamson, A. W. Purcell, N. L. Dudek, M. J. McConville, R. A. O'Hair, G. N. Khairallah, D. I. Godfrey, D. P. Fairlie, J. Rossjohn, and J. McCluskey. 2012. MR1 presents microbial vitamin B metabolites to MAIT cells. *Nature* 491: 717-723.
6. Gapin, L. 2014. Check MAIT. *J Immunol* 192: 4475-4480.
7. Slichter, C. K., A. McDavid, H. W. Miller, G. Finak, B. J. Seymour, J. P. McNevin, G. Diaz, J. L. Czartoski, M. J. McElrath, R. Gottardo, and M. Prlic. 2016. Distinct activation thresholds of human conventional and innate-like memory T cells. *JCI insight* 1.
8. Lamichhane, R., M. Schneider, S. M. de la Harpe, T. W. R. Harrop, R. F. Hannaway, P. K. Dearden, J. R. Kirman, J. D. A. Tyndall, A. J. Vernall, and J. E. Ussher. 2019. TCR- or Cytokine-Activated CD8. *Cell reports* 28: 3061-3076.e3065.
9. Kedia-Mehta, N., and A. E. Hogan. 2022. MAITabolism(2) - the emerging understanding of MAIT cell metabolism and their role in metabolic disease. *Front Immunol* 13: 1108071.
10. Zinser, M. E., A. J. Highton, A. Kurioka, B. Kronsteiner, J. Hagel, T. Leng, E. Marchi, C. Phetsouphanh, C. B. Willberg, S. J. Dunachie, and P. Klenerman. 2018. Human MAIT cells show metabolic quiescence with rapid glucose-dependent upregulation of granzyme B upon stimulation. *Immunol Cell Biol*.
11. O'Brien, A., R. M. Loftus, M. M. Pisarska, L. M. Tobin, R. Bergin, N. A. W. Wood, C. Foley, A. Mat, F. C. Tinley, C. Bannan, G. Sommerville, N. Veerapen, G. S. Besra, L. V. Sinclair, P. N. Moynagh, L. Lynch, D. K. Finlay, D. O'Shea, and A. E. Hogan. 2019. Obesity Reduces mTORC1 Activity in Mucosal-Associated Invariant T Cells, Driving Defective Metabolic and Functional Responses. *J Immunol* 202: 3404-3411.
12. Kedia-Mehta, N., M. M. Pisarska, C. Rollings, C. O'Neill, C. De Barra, C. Foley, N. A. W. Wood, N. Wrigley-Kelly, N. Veerapen, G. Besra, R. Bergin, N. Jones, D. O'Shea, L. V. Sinclair, and A. E. Hogan. 2023. The proliferation of human mucosal-associated invariant T cells requires a MYC-SLC7A5-glycolysis metabolic axis. *Sci Signal* 16: eabo2709.

13. Riffelmacher, T., M. Paynich Murray, C. Wientjens, S. Chandra, V. Cedillo-Castelan, T. F. Chou, S. McArdle, C. Dillingham, J. Devereaux, A. Nilsen, S. Brunel, D. M. Lewinsohn, J. Hasty, G. Seumois, C. A. Benedict, P. Vijayanand, and M. Kronenberg. 2023. Divergent metabolic programmes control two populations of MAIT cells that protect the lung. *Nat Cell Biol* 25: 877-891.
14. Brien, A. O., N. Kedia-Mehta, L. Tobin, N. Veerapen, G. S. Besra, D. O. Shea, and A. E. Hogan. 2020. Targeting mitochondrial dysfunction in MAIT cells limits IL-17 production in obesity. *Cell Mol Immunol*.
15. Haschka, D., A. Hoffmann, and G. Weiss. 2021. Iron in immune cell function and host defense. *Seminars in cell & developmental biology* 115: 27-36.
16. Payne, S. M. 1993. Iron acquisition in microbial pathogenesis. *Trends in microbiology* 1: 66-69.
17. Nemeth, E., M. S. Tuttle, J. Powelson, M. B. Vaughn, A. Donovan, D. M. Ward, T. Ganz, and J. Kaplan. 2004. Hepcidin regulates cellular iron efflux by binding to ferroportin and inducing its internalization. *Science* 306: 2090-2093.
18. Nemeth, E., S. Rivera, V. Gabayan, C. Keller, S. Taudorf, B. K. Pedersen, and T. Ganz. 2004. IL-6 mediates hypoferremia of inflammation by inducing the synthesis of the iron regulatory hormone hepcidin. *J Clin Invest* 113: 1271-1276.
19. Yarosz, E. L., C. Ye, A. Kumar, C. Black, E. K. Choi, Y. A. Seo, and C. H. Chang. 2020. Cutting Edge: Activation-Induced Iron Flux Controls CD4 T Cell Proliferation by Promoting Proper IL-2R Signaling and Mitochondrial Function. *J Immunol* 204: 1708-1713.
20. Frost, J. N., T. K. Tan, M. Abbas, S. K. Wideman, M. Bonadonna, N. U. Stoffel, K. Wray, B. Kronsteiner, G. Smits, D. R. Campagna, T. L. Duarte, J. M. Lopes, A. Shah, A. E. Armitage, J. Arezes, P. J. Lim, A. E. Preston, D. Ahern, M. Teh, C. Naylor, M. Salio, U. Gileadi, S. C. Andrews, S. J. Dunachie, M. B. Zimmermann, F. R. M. van der Klis, V. Cerundolo, O. Bannard, S. J. Draper, A. R. M. Townsend, B. Galy, M. D. Fleming, M. C. Lewis, and H. Drakesmith. 2021. Hepcidin-Mediated Hypoferremia Disrupts Immune Responses to Vaccination and Infection. *Med (N Y)* 2: 164-179 e112.
21. Andreini, C., V. Putignano, A. Rosato, and L. Banci. 2018. The human iron-proteome. *Metallomics* 10: 1223-1231.
22. Teh, M. R., J. N. Frost, A. E. Armitage, and H. Drakesmith. 2021. Analysis of Iron and Iron-Interacting Protein Dynamics During T-Cell Activation. *Front Immunol* 12: 714613.
23. Mookerjee, S. A., A. A. Gerencser, D. G. Nicholls, and M. D. Brand. 2017. Quantifying intracellular rates of glycolytic and oxidative ATP production and consumption using extracellular flux measurements. *J Biol Chem* 292: 7189-7207.
24. Jenkins, B. J., J. Blagih, F. M. Ponce-Garcia, M. Canavan, N. Gudgeon, S. Eastham, D. Hill, M. M. Hanlon, E. H. Ma, E. L. Bishop, A. Rees, J. G. Cronin, E. C. Jury, S. K. Dimeloe, D. J. Veale, C. A. Thornton, K. H. Vousden, D. K. Finlay, U. Fearon, G. W. Jones, L. V. Sinclair, E. E. Vincent, and N. Jones. 2023. Canagliflozin impairs T cell effector function via metabolic suppression in autoimmunity. *Cell Metab* 35: 1132-1146 e1139.
25. Arguello, R. J., A. J. Combes, R. Char, J. P. Gigan, A. I. Baaziz, E. Bousiquot, V. Camosseto, B. Samad, J. Tsui, P. Yan, S. Boissonneau, D. Figarella-Branger, E. Gatti, E. Tabouret, M. F. Krummel, and P. Pierre. 2020. SCENITH: A Flow

Cytometry-Based Method to Functionally Profile Energy Metabolism with Single-Cell Resolution. *Cell Metab* 32: 1063-1075 e1067.
26. Provine, N. M., and P. Klenerman. 2020. MAIT Cells in Health and Disease. *Annu Rev Immunol* 38: 203-228.
27. Meierovics, A., W. J. Yankelevich, and S. C. Cowley. 2013. MAIT cells are critical for optimal mucosal immune responses during in vivo pulmonary bacterial infection. *Proc Natl Acad Sci U S A* 110: E3119-3128.
28. Meermeier, E. W., C. L. Zheng, J. G. Tran, S. Soma, A. H. Worley, D. I. Weiss, R. L. Modlin, G. Swarbrick, E. Karamooz, S. Khuzwayo, E. B. Wong, M. C. Gold, and D. M. Lewinsohn. 2022. Human lung-resident mucosal-associated invariant T cells are abundant, express antimicrobial proteins, and are cytokine responsive. *Commun Biol* 5: 942.
29. van Wilgenburg, B., L. Loh, Z. Chen, T. J. Pediongco, H. Wang, M. Shi, Z. Zhao, M. Koutsakos, S. Nüssing, S. Sant, Z. Wang, C. D'Souza, X. Jia, C. F. Almeida, L. Kostenko, S. B. G. Eckle, B. S. Meehan, A. Kallies, D. I. Godfrey, P. C. Reading, A. J. Corbett, J. McCluskey, P. Klenerman, K. Kedzierska, and T. S. C. Hinks. 2018. MAIT cells contribute to protection against lethal influenza infection in vivo. *Nature communications* 9: 4706.
30. O'Neill, L. A., R. J. Kishton, and J. Rathmell. 2016. A guide to immunometabolism for immunologists. *Nat Rev Immunol* 16: 553-565.
31. Cassidy, F. C., N. Kedia-Mehta, R. Bergin, A. Woodcock, A. Berisha, B. Bradley, E. Booth, B. J. Jenkins, O. K. Ryan, N. Jones, L. V. Sinclair, D. O'Shea, and A. E. Hogan. 2023. Glycogen-fuelled metabolism supports rapid mucosal-associated invariant T cell responses. *Proc Natl Acad Sci U S A* 120: e2300566120.
32. Harding, C., J. Heuser, and P. Stahl. 1983. Receptor-mediated endocytosis of transferrin and recycling of the transferrin receptor in rat reticulocytes. *J Cell Biol* 97: 329-339.
33. Howden, A. J. M., J. L. Hukelmann, A. Brenes, L. Spinelli, L. V. Sinclair, A. I. Lamond, and D. A. Cantrell. 2019. Quantitative analysis of T cell proteomes and environmental sensors during T cell differentiation. *Nat Immunol* 20: 1542-1554.
34. Littwitz-Salomon, E., D. Moreira, J. N. Frost, C. Choi, K. T. Liou, D. K. Ahern, S. O'Shaughnessy, B. Wagner, C. A. Biron, H. Drakesmith, U. Dittmer, and D. K. Finlay. 2021. Metabolic requirements of NK cells during the acute response against retroviral infection. *Nature communications* 12: 5376.
35. Jabara, H. H., S. E. Boyden, J. Chou, N. Ramesh, M. J. Massaad, H. Benson, W. Bainter, D. Fraulino, F. Rahimov, C. Sieff, Z. J. Liu, S. H. Alshemmari, B. K. Al-Ramadi, H. Al-Dhekri, R. Arnaout, M. Abu-Shukair, A. Vatsayan, E. Silver, S. Ahuja, E. G. Davies, M. Sola-Visner, T. K. Ohsumi, N. C. Andrews, L. D. Notarangelo, M. D. Fleming, W. Al-Herz, L. M. Kunkel, and R. S. Geha. 2016. A missense mutation in TFRC, encoding transferrin receptor 1, causes combined immunodeficiency. *Nat Genet* 48: 74-78.
36. Preston, G. C., L. V. Sinclair, A. Kaskar, J. L. Hukelmann, M. N. Navarro, I. Ferrero, H. R. MacDonald, V. H. Cowling, and D. A. Cantrell. 2015. Single cell tuning of Myc expression by antigen receptor signal strength and interleukin-2 in T lymphocytes. *The EMBO journal* 34: 2008-2024.
37. Souter, M. N. T., W. Awad, S. Li, T. J. Pediongco, B. S. Meehan, L. J. Meehan, Z. Tian, Z. Zhao, H. Wang, A. Nelson, J. Le Nours, Y. Khandokar, T. Praveena, J. Wubben, J. Lin, L. C. Sullivan, G. O. Lovrecz, J. Y. W. Mak, L. Liu, L.

Kostenko, K. Kedzierska, A. J. Corbett, D. P. Fairlie, A. G. Brooks, N. A. Gherardin, A. P. Uldrich, Z. Chen, J. Rossjohn, D. I. Godfrey, J. McCluskey, D. G. Pellicci, and S. B. G. Eckle. 2022. CD8 coreceptor engagement of MR1 enhances antigen responsiveness by human MAIT and other MR1-reactive T cells. *J Exp Med* 219.

38. Torti, F. M., and S. V. Torti. 2002. Regulation of ferritin genes and protein. *Blood* 99: 3505-3516.

39. Keberle, H. 1964. The Biochemistry of Desferrioxamine and Its Relation to Iron Metabolism. *Ann N Y Acad Sci* 119: 758-768.

40. Voss, K., A. E. Sewell, E. S. Krystofiak, K. N. Gibson-Corley, A. C. Young, J. H. Basham, A. Sugiura, E. N. Arner, W. N. Beavers, D. E. Kunkle, M. E. Dickson, G. A. Needle, E. P. Skaar, W. K. Rathmell, M. J. Ormseth, A. S. Major, and J. C. Rathmell. 2023. Elevated transferrin receptor impairs T cell metabolism and function in systemic lupus erythematosus. *Sci Immunol* 8: eabq0178.

41. Golonka, R., B. S. Yeoh, and M. Vijay-Kumar. 2019. The Iron Tug-of-War between Bacterial Siderophores and Innate Immunity. *J Innate Immun* 11: 249-262.

42. Le Bourhis, L., M. Dusseaux, A. Bohineust, S. Bessoles, E. Martin, V. Premel, M. Core, D. Sleurs, N. E. Serriari, E. Treiner, C. Hivroz, P. Sansonetti, M. L. Gougeon, C. Soudais, and O. Lantz. 2013. MAIT cells detect and efficiently lyse bacterially-infected epithelial cells. *PLoS Pathog* 9: e1003681.

43. Cooper, A. J. R., J. Clegg, F. C. Cassidy, A. E. Hogan, and R. M. McLoughlin. 2022. Human MAIT Cells Respond to Staphylococcus aureus with Enhanced Anti-Bacterial Activity. *Microorganisms* 10.

44. Boulouis, C., W. R. Sia, M. Y. Gulam, J. Q. M. Teo, Y. T. Png, T. K. Phan, J. Y. W. Mak, D. P. Fairlie, I. K. H. Poon, T. H. Koh, P. Bergman, C. M. Lim, L. F. Wang, A. L. H. Kwa, J. K. Sandberg, and E. Leeansyah. 2020. Human MAIT cell cytolytic effector proteins synergize to overcome carbapenem resistance in Escherichia coli. *PLoS Biol* 18: e3000644.

45. Chen, Z., H. Wang, C. D'Souza, S. Sun, L. Kostenko, S. B. Eckle, B. S. Meehan, D. C. Jackson, R. A. Strugnell, H. Cao, N. Wang, D. P. Fairlie, L. Liu, D. I. Godfrey, J. Rossjohn, J. McCluskey, and A. J. Corbett. 2017. Mucosal-associated invariant T-cell activation and accumulation after in vivo infection depends on microbial riboflavin synthesis and co-stimulatory signals. *Mucosal Immunol* 10: 58-68.

46. Lopez-Rodriguez, J. C., S. J. Hancock, K. Li, S. Crotta, C. Barrington, A. Suarez-Bonnet, S. L. Priestnall, J. Aube, A. Wack, P. Klenerman, J. A. Bengoechea, and P. Barral. 2023. Type I interferons drive MAIT cell functions against bacterial pneumonia. *J Exp Med* 220.

47. Wang, H., C. D'Souza, X. Y. Lim, L. Kostenko, T. J. Pediongco, S. B. G. Eckle, B. S. Meehan, M. Shi, N. Wang, S. Li, L. Liu, J. Y. W. Mak, D. P. Fairlie, Y. Iwakura, J. M. Gunnersen, A. W. Stent, D. I. Godfrey, J. Rossjohn, G. P. Westall, L. Kjer-Nielsen, R. A. Strugnell, J. McCluskey, A. J. Corbett, T. S. C. Hinks, and Z. Chen. 2018. MAIT cells protect against pulmonary Legionella longbeachae infection. *Nature communications* 9: 3350.

48. Crouch, M. L., M. Castor, J. E. Karlinsey, T. Kalhorn, and F. C. Fang. 2008. Biosynthesis and IroC-dependent export of the siderophore salmochelin are essential for virulence of Salmonella enterica serovar Typhimurium. *Molecular microbiology* 67: 971-983.

49. Bachman, M. A., V. L. Miller, and J. N. Weiser. 2009. Mucosal lipocalin 2 has pro-inflammatory and iron-sequestering effects in response to bacterial enterobactin. *PLoS Pathog* 5: e1000622.
50. Cianciotto, N. P. 2015. An update on iron acquisition by Legionella pneumophila: new pathways for siderophore uptake and ferric iron reduction. *Future Microbiol* 10: 841-851.
51. Howson, L. J., G. Napolitani, D. Shepherd, H. Ghadbane, P. Kurupati, L. Preciado-Llanes, M. Rei, H. C. Dobinson, M. M. Gibani, K. W. W. Teng, E. W. Newell, N. Veerapen, G. S. Besra, A. J. Pollard, and V. Cerundolo. 2018. MAIT cell clonal expansion and TCR repertoire shaping in human volunteers challenged with Salmonella Paratyphi A. *Nature communications* 9: 253.

Figure Legends

Figure 1. MAIT cells increase CD71 and transferrin uptake upon activation. (A-D) Flow cytometric dot plots, scatter plots, and representative flow cytometric histograms showing CD71 expression in MAIT cells, basal or stimulated for 18 hr with anti-CD3/CD28 TCR beads and IL-18. (E) Scatter plot comparing CD71 expression on MAIT cells and conventional T cells (non-MAIT CD3+ cells) after 18 hours stimulation with anti-CD3/CD28 TCR beads and IL-18. (F-H) Flow cytometric dot plots, scatter plots, and representative flow cytometric histograms showing CD71 expression in MAIT cells, basal or stimulated for 18 hr with anti-CD3/CD28 TCR beads and IL-18, in the absence or presence of the iron chelator, deferoxamine (DFO). (I-L) Flow cytometric dot plots, scatter plots, and representative flow-cytometric histograms showing transferrin content in MAIT cells, basal or stimulated for 18 hr with anti-CD3/CD28 TCR beads and IL-18. (M) Scatter plot comparing transferrin uptake by MAIT cells and conventional T cells (non-MAIT CD3+ cells) after 18 hours stimulation with anti-CD3/CD28 TCR beads and IL-18. (N) Correlation plot showing the relationship between CD71 expression and Transferrin uptake in activated MAIT cells (18 hr with anti-CD3/CD28 TCR beads and IL-18). * $p<0.05$, ** $p<0.01$, *** $p<0.001$ and **** $p<0.0001$.

Figure 2. MAIT cells store and utilize iron. (A and B). Scatter plot showing protein copy number of the heavy and light chain subunits of ferritin in IL-2 expanded MAIT cells, basal or stimulated for 18 hr with anti-CD3/CD28 TCR beads and IL-18. (C) Heat map of iron-related protein content in IL-2 expanded MAIT cells, basal or stimulated for 18 hr with anti-CD3/CD28 TCR beads and IL-18. (D) Pie graph showing proportional pathway analysis based on iron-related protein content in MAIT cells (analysis performed with Panther). (E-G) Estimated iron, heme and iron-sulphur cluster atoms extrapolated from proteome of IL-2 expanded MAIT cells, basal or stimulated for 18 hr with anti-CD3/CD28 TCR beads and IL-18. * $p<0.05$.

Figure 3. Iron restriction alters MAIT cells metabolism. (A-D) Representative flow cytometric histograms and scatter plots showing puromycin incorporation in MAIT cells, basal or stimulated for 18 hr with anti-CD3/CD28 TCR beads and IL-18, in the absence or presence of the iron chelator, deferoxamine (DFO). (E) Scatter plot

showing percentage dependency on glucose metabolism in MAIT cells stimulated for 18 hr with anti-CD3/CD28 TCR beads and IL-18, in the presence or absence of DFO. (F) Scatter plot showing percentage dependency on fatty acid oxidation and amino acid oxidation in MAIT cells stimulated for 18 hr with anti-CD3/CD28 TCR beads and IL-18, in the presence or absence of DFO. (G and H) Scatter plots showing the mean-fluorescence intensity (MFI) of Mitotracker Green and Mitotracker Deep Red , depicting mitochondrial mass and mitochondrial membrane potential, respectively, in MAIT cells stimulated with anti-CD3/CD28 TCR beads and IL-18 for 18hr, in the presence or absence of DFO. (I-J) Representative seahorse trace and scatter plot showing oxygen consumption rates (OCR) in MAIT cells stimulated with anti-CD3/CD28 TCR beads and IL-18 for 24hr, in the presence or absence of DFO. (K) Scatter plot showing the mitochondrial capacity (post FCCP treatment) in MAIT cells stimulated with anti-CD3/CD28 TCR beads and IL-18 for 24hr, in the presence or absence of DFO. (L) Scatter plot showing the impact of an anti-CD71 monoclonal with blocking activity on ATP production in MAIT cells stimulated with anti-CD3/CD28 TCR beads and IL-18 for 18hr. * $p<0.05$, ** $p<0.01$, *** $p<0.001$ and **** $p<0.0001$.

Figure 4. MAIT cells require iron for their functional responses. (A) Representative flow cytometry histogram and scatter plot showing IFN-γ levels (mean fluorescence intensity (MFI)) in MAIT cells stimulated with anti-CD3/CD28 TCR beads and IL-18 for 18hr, in the absence or presence of the iron chelator, deferoxamine (DFO) measured by flow cytometry. (B-D) Scatter plots showing IFN-γ, IL-17 and IL-2 secreted protein levels (normalised to assay) in IL-2 expanded MAIT cells stimulated with anti-CD3/CD28 TCR beads and IL-18 for 18hr, in the absence or presence DFO, as measured by ELISA. (E and F) Scatter plots showing the impact of an anti-CD71 monoclonal with blocking activity on IFN-γ and IL-26 secreted protein levels (normalised to assay) in IL-2 expanded MAIT cells stimulated with anti-CD3/CD28 TCR beads and IL-18 for 18hr, as measured by ELISA. (G-H) Line graph showing IFN-γ or granzyme B levels (percentage of parent population) in MAIT cells co-cultured at 1:1 ratio with THP-1 cells alone or pre-pulsed with fixed *E. coli* (DH5α) for 18hr, in the absence or presence of the anti-CD71 monoclonal with blocking activity, as measured by flow cytometry. (I) Scatter plot showing the impact of the ATP-synthase inhibitor, oligomycin, on MAIT

cell proliferative capacity (during a 5 day IL-2 mediated MAIT cell expansion culture), whereby the mean fluorescence intensity (MFI) of the intracellular dye CellTrace Violet decreases with each cycle of cell division. (J and K) Scatter plots showing the impact of long-term iron depletion via DFO, and alternative iron repletion via Iron(II) sulfate heptahydrate ($FeSO_4 \bullet 7H_2O$) on MAIT cell proliferation and viability, during a 5 day IL-2 mediated MAIT cell expansion culture. * $p<0.05$, ** $p<0.01$ and *** $p<0.001$.

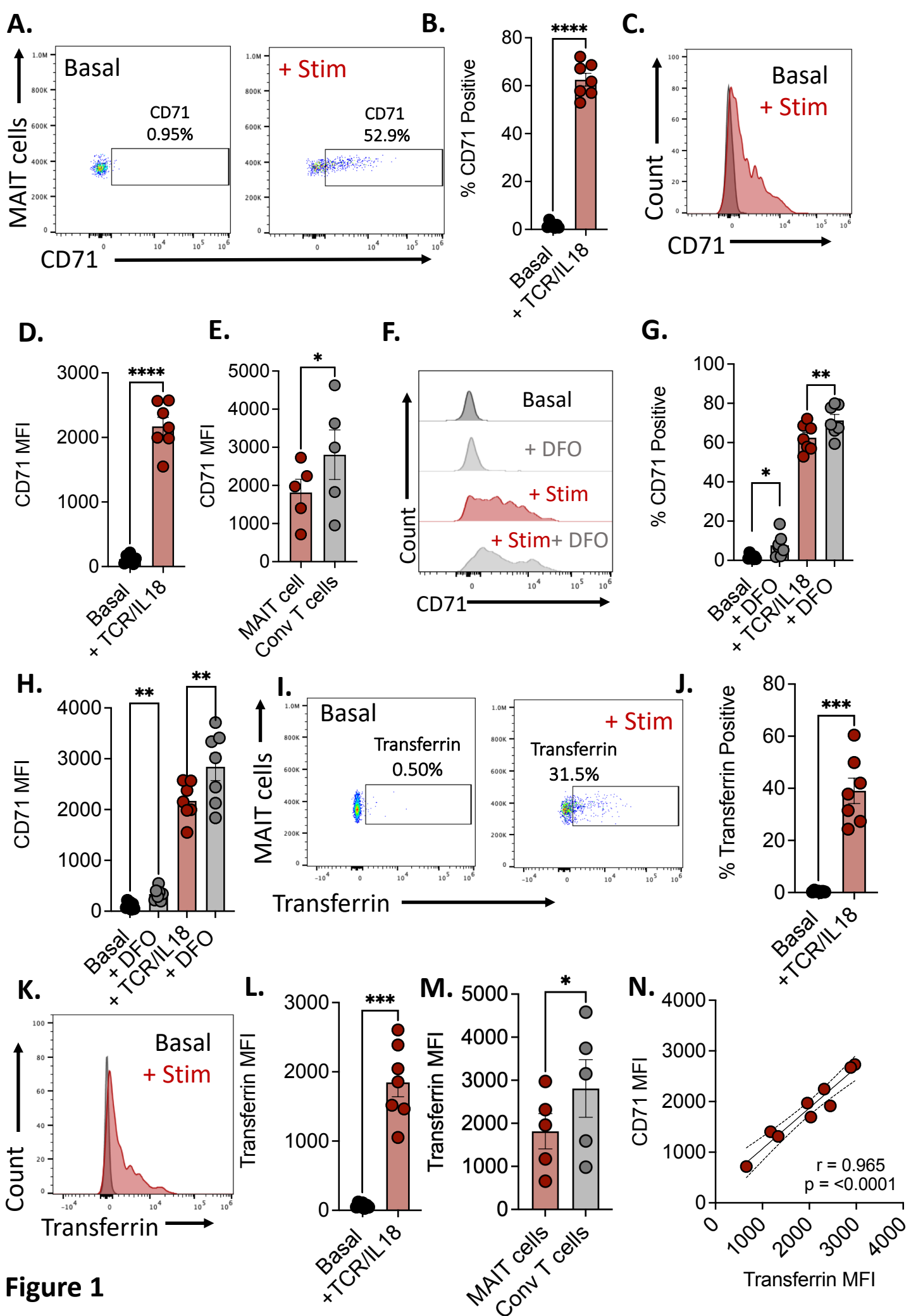
A.
Basal
CD71
0.95%
+ Stim
CD71
52.9%
MAIT cells
CD71
B.
% CD71 Positive
****
Basal
+ TCR/IL18
C.
Basal
+ Stim
Count
CD71
D.
CD71 MFI
****
Basal
+ TCR/IL18
E.
CD71 MFI
*
MAIT cell
Conv T cells
F.
Basal
+ DFO
+ Stim
+ Stim+ DFO
Count
CD71
G.
% CD71 Positive
*
**
Basal
+ DFO
+ TCR/IL18
+ DFO
H.
CD71 MFI
**
**
Basal
+ DFO
+ TCR/IL18
+ DFO
I.
Basal
Transferrin
0.50%
+ Stim
Transferrin
31.5%
MAIT cells
Transferrin
J.
% Transferrin Positive
***
Basal
+TCR/IL18
K.
Basal
+ Stim
Count
Transferrin
L.
Transferrin MFI
***
Basal
+TCR/IL18
M.
Transferrin MFI
*
MAIT cells
Conv T cells
N.
CD71 MFI
r = 0.965
p = <0.0001
Transferrin MFI

Figure 1

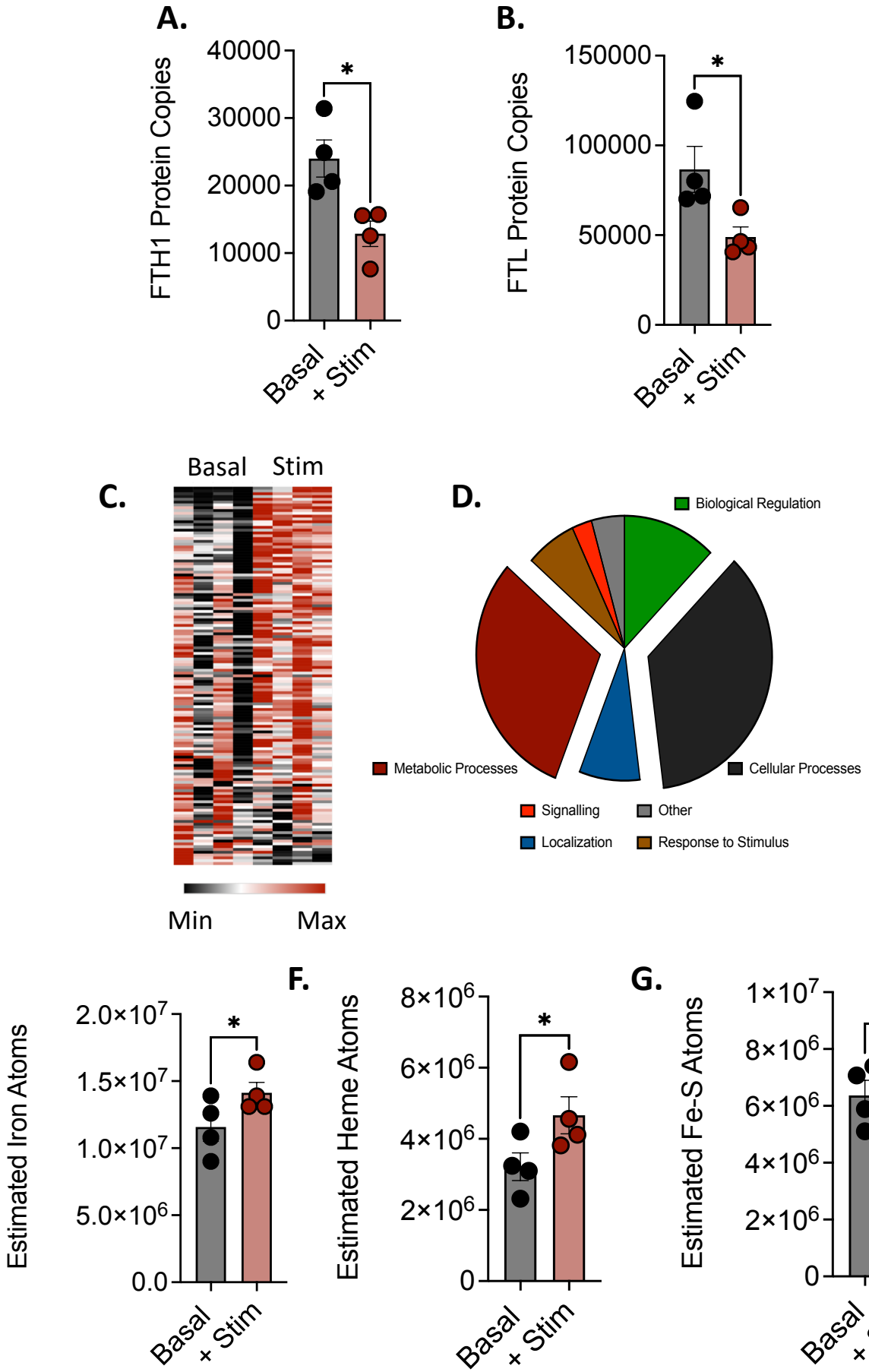
A.
FTH1 Protein Copies
40000
30000
20000
10000
0
*
Basal
+ Stim
B.
FTL Protein Copies
150000
100000
50000
0
*
Basal
+ Stim
C.
Basal
Stim
Min
Max
D.
Biological Regulation
Metabolic Processes
Cellular Processes
Signalling
Other
Localization
Response to Stimulus
E.
Estimated Iron Atoms
2.0×10^7
1.5×10^7
1.0×10^7
5.0×10^6
0.0
*
Basal
+ Stim
F.
Estimated Heme Atoms
8×10^6
6×10^6
4×10^6
2×10^6
0
*
Basal
+ Stim
G.
Estimated Fe-S Atoms
1×10^7
8×10^6
6×10^6
4×10^6
2×10^6
0
*
Basal
+ Stim

Figure 2

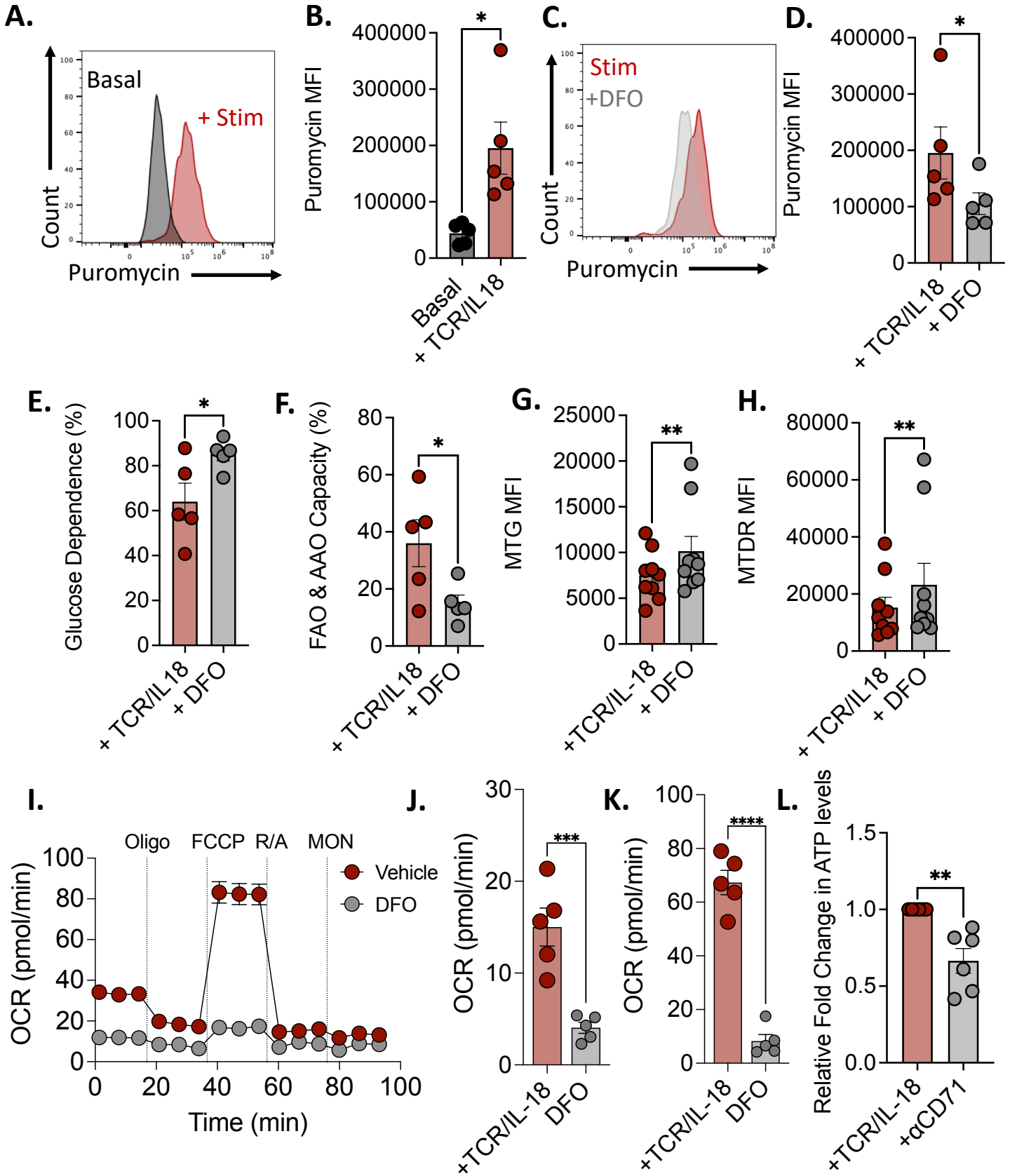
A.
Basal
+ Stim
Count
Puromycin
B.
Puromycin MFI
400000
300000
200000
100000
0
*
Basal
+ TCR/IL18
C.
Stim
+DFO
Count
Puromycin
D.
Puromycin MFI
400000
300000
200000
100000
0
*
+ TCR/IL18
+ DFO
E.
Glucose Dependence (%)
100
80
60
40
20
0
*
+ TCR/IL18
+ DFO
F.
FAO & AAO Capacity (%)
80
60
40
20
0
*
+ TCR/IL18
+ DFO
G.
MTG MFI
25000
20000
15000
10000
5000
0
**
+TCR/IL-18
+ DFO
H.
MTDR MFI
80000
60000
40000
20000
0
**
+ TCR/IL18
+ DFO
I.
OCR (pmol/min)
100
80
60
40
20
0
Oligo
FCCP
R/A
MON
Vehicle
DFO
0
20
40
60
80
100
Time (min)
J.
OCR (pmol/min)
30
20
10
0
***
+TCR/IL-18
DFO
K.
OCR (pmol/min)
100
80
60
40
20
0
****
+TCR/IL-18
DFO
L.
Relative Fold Change in ATP levels
1.5
1.0
0.5
0.0
**
+TCR/IL-18
+αCD71

Figure 3

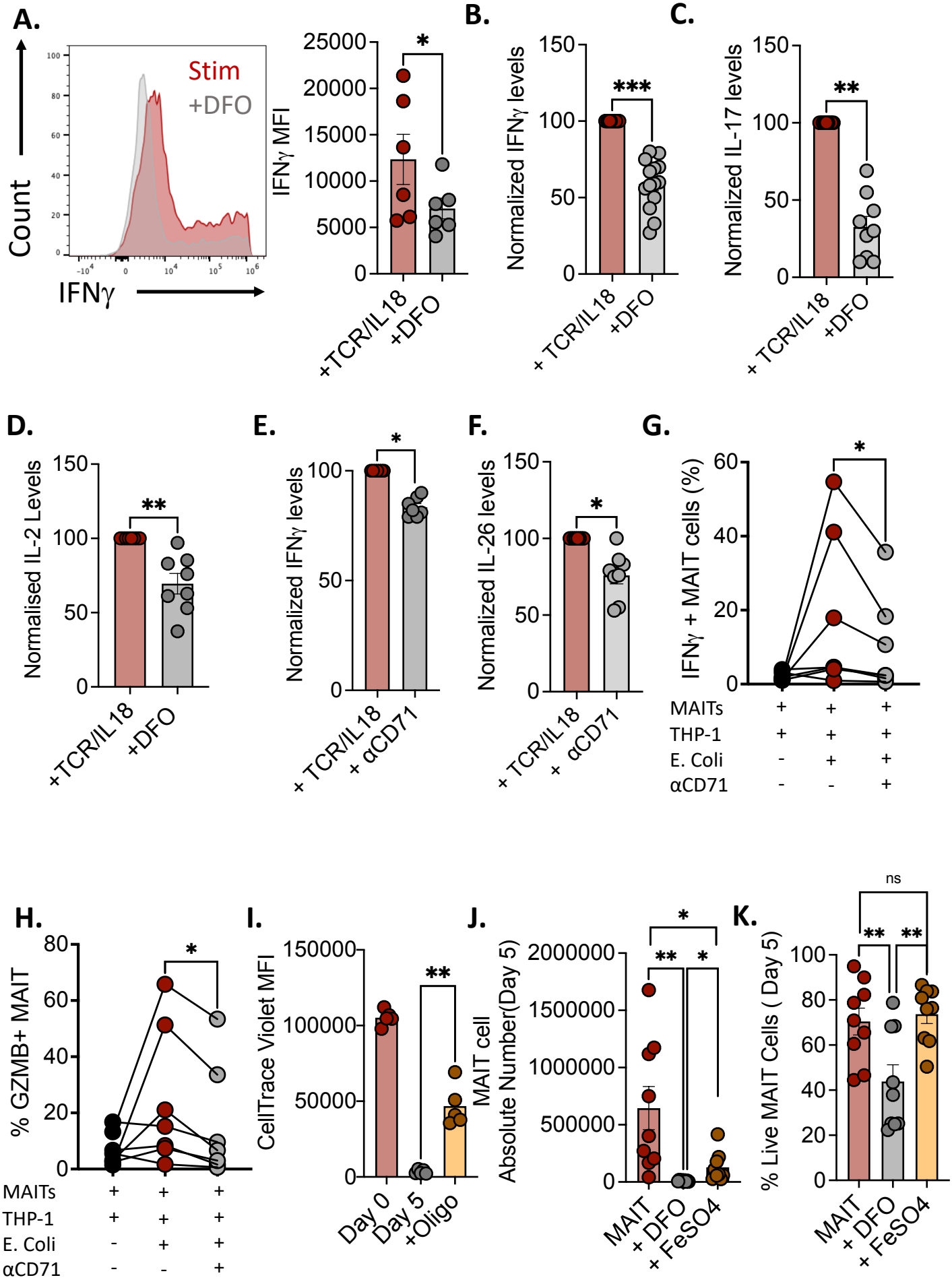
A.
Stim
+DFO
Count
IFNγ
IFNγ MFI
+TCR/IL18
+DFO
B.
Normalized IFNγ levels
+ TCR/IL18
+DFO
C.
Normalized IL-17 levels
+ TCR/IL18
+DFO
D.
Normalised IL-2 Levels
+TCR/IL18
+DFO
E.
Normalized IFNγ levels
+ TCR/IL18
+ αCD71
F.
Normalized IL-26 levels
+ TCR/IL18
+ αCD71
G.
IFNγ + MAIT cells (%)
MAITs + + +
THP-1 + + +
E. Coli - + +
αCD71 - - +
H.
% GZMB+ MAIT
MAITs + + +
THP-1 + + +
E. Coli - + +
αCD71 - - +
I.
CellTrace Violet MFI
Day 0
Day 5
+Oligo
J.
MAIT cell Absolute Number(Day 5)
MAIT
+ DFO
+ FeSO4
K.
ns
% Live MAIT Cells (Day 5)
MAIT
+ DFO
+ FeSO4

Figure 4

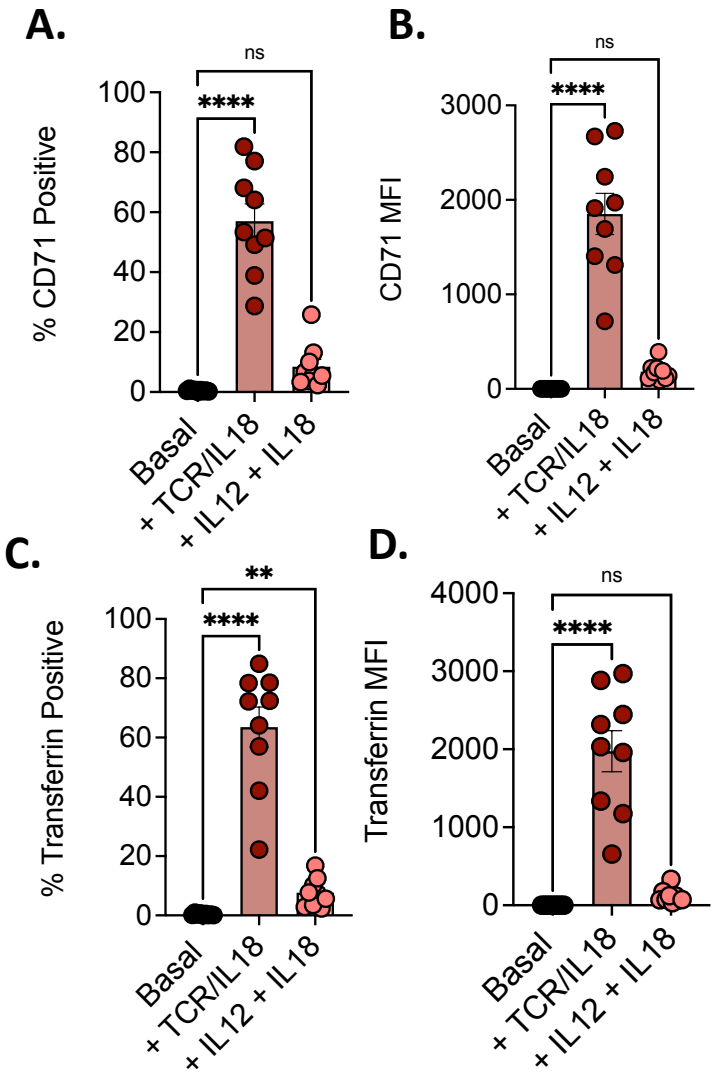

Figure S1: (A-D) Scatter plots showing CD71 expression (both % and MFI) on MAIT cells basally or after 18 hours stimulation with either TCR beads and IL-18 (50ng/ml) or IL-12/IL-18 (both 50ng/ml).

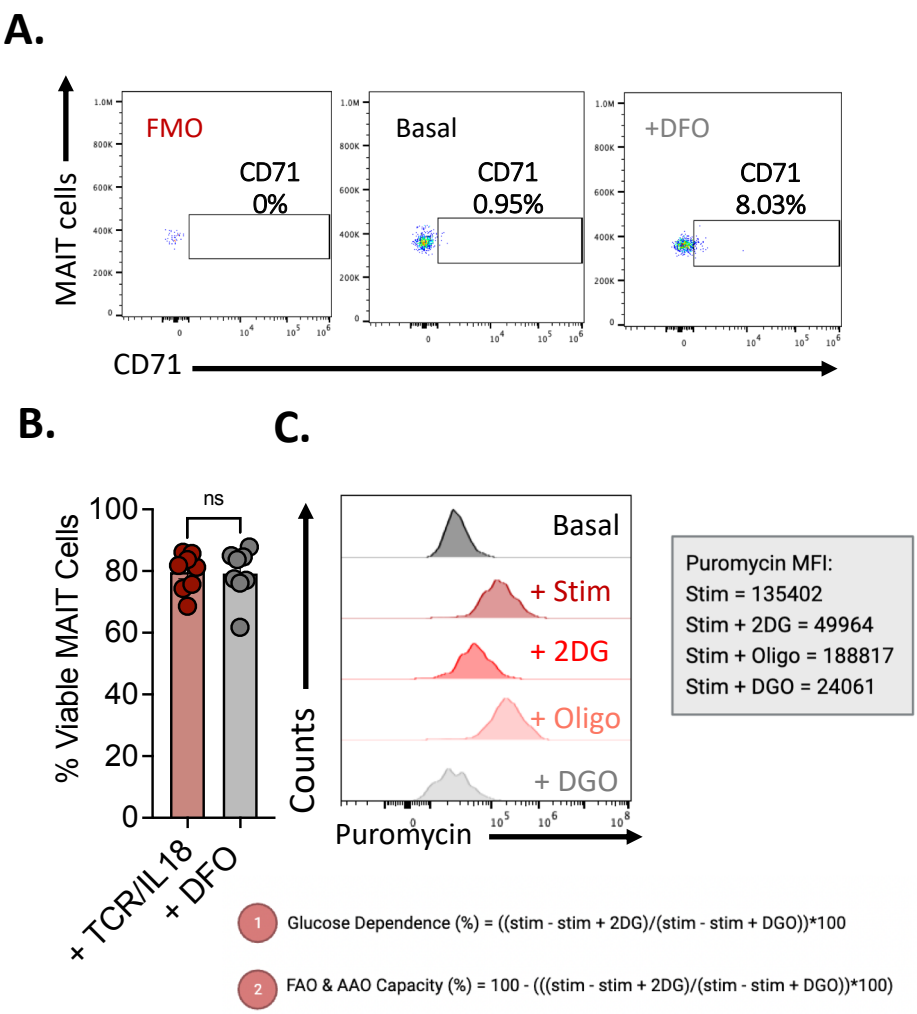

Figure S2: (A) Representative flow cytometry dot plots detailing CD71 expression on MAIT cells basally or after 18 hours of DFO treatment (200μM), including flow minus one (FMO) control for CD71. (B) Scatter plot showing the viability of TCR/IL-18 activated MAIT cells in the absence or presence of DFO (200μM) for 18 hours. (C) Representative example of SCENITH data including calculations for presented metabolic dependencies. (ns = not significant)

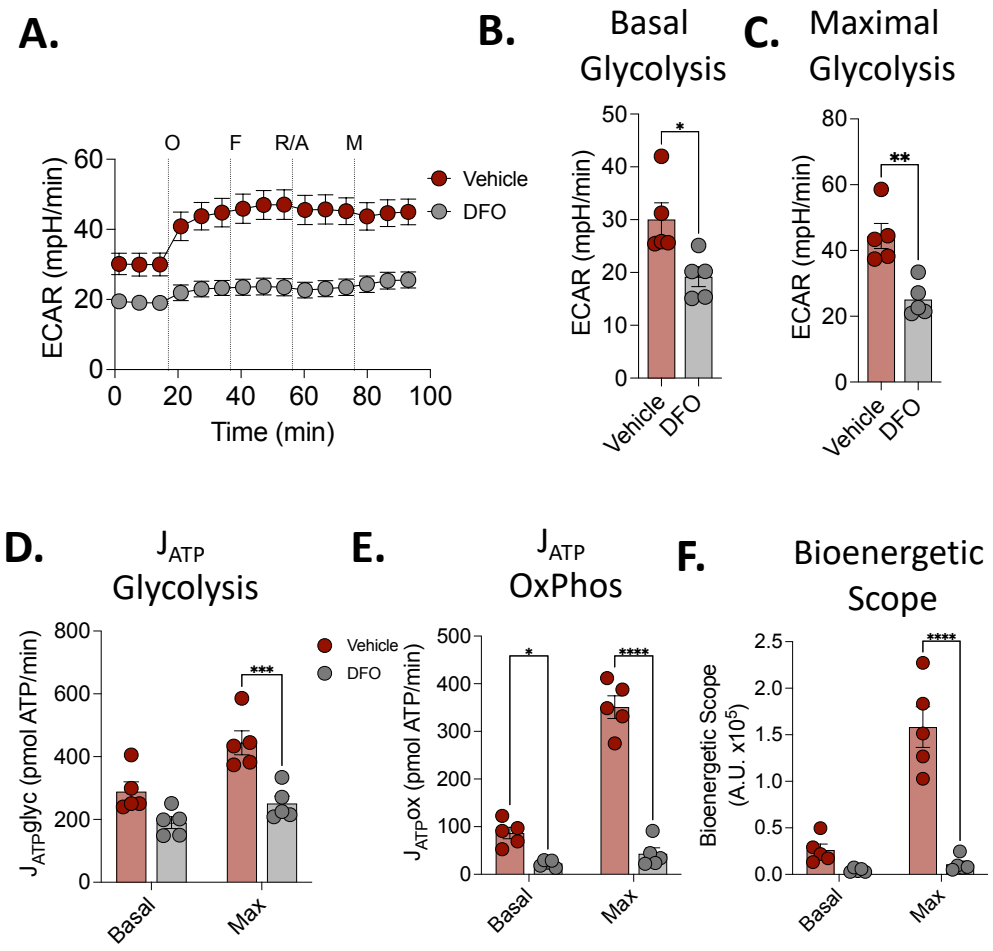

Figure S3: (A) Representative Seahorse trace showing extracellular acidification rate (ECAR) following pre-optimized injections of oligomycin, FCCP, antimycin A/rotenone (all 1 μM) and monensin (20μM) in MAIT cells activated for 18 hours in the absence or presence of DFO (200μM). (B-C) Scatter plots showing basal or maximal glycolytic rates in MAIT cells activated for 18 hours in the absence or presence of DFO (200μM). (D-E) Scatter plots showing basal or maximal ATP (J_{ATP}) production linked to glycolysis or oxidative phosphorylation in MAIT cells activated for 18 hours in the absence or presence of DFO (200μM). (F) Scatter plot showing basal or maximal bioenergetic scope of MAIT cells activated for 18 hours in the absence or presence of DFO (200μM).

Table S1: List of iron-interacting proteins

Identifier			
BOLA2	ISCA2	SDHC	FTL
ACO2	PRIM2	CYP51A1	METAP2
UQCRFS1	ISCU	CYB5A	PPP3CA
CISD2	ABAT	PTGES2	METAP1
NDUFS1	NFS1	CYP20A1	RRM2
ABCE1	GLRX5	CYBA	MRE11
SDHB	NFU1	HPX	ADO
NDUFV2	ACO1	NENF	OSGEP
CISD1	DPH2	TBXAS1	P4HA1
NDUFV1	DPYD	RORC	KDM2A
GLRX3	POLA1	SDHD	ALKBH5
NUBP2	NTHL1	JAK3	NIF3L1
NDUFS8	DPH1	HEBP1	FTO
NDUFS2	POLE	MT-CO1	JMJD6
CIAPIN1	ABCB7	PTGIS	RIOX1
NUBP1	FECH	COX15	HPDL
ERCC2	HBA1	HMOX1	MSMO1
NDUFS7	HBB	CYB5R4	RRM2B
POLD1	CYCS	MT-CYB	FTH1
FDX1	ALB	FADS2	RIOX2
ETFDH	CYB5B	INPPL1	PPP3CB
CISD3	COPA	DGCR8	LTF
ELP3	CYC1	HERC2	DOHH
PPAT	PGRMC2	ABCB6	PPP3CC
CDKAL1	HMOX2	AFM	EGLN1
KDM2B	COX5A	CYP4F22	RPE
ASPHD2	CAT	GSTP1	KDM3B
KDM5A	PGRMC1	PPP1CA	PHF8
KDM5B	HCCS	ETHE1	PIR
KDM4A	HEBP2	FXN	OGFOD1
KDM4B	KDM3A	TMPPE	SCD
PHF2	P4HA2	KDM6B	PLOD3
ACP5	SCD5	HIF1AN	ADI1
P3H1	KDM5C	GALT	